Aerothermal Effects Of Reentry On A Generic Geometry – A Continuum Approach

Enes Çelik[1]
Department of Aeronautical/Astronautical Engineering, Istanbul Technical University

I.Abstract

The design of hypersonic air vehicles must take into account the aerothermodynamic loads caused by shock wave boundary layer interactions (shock interactions). The accuracy of the Computational Fluid Dynamics (CFD) software SU2-NEMO in predicting these hypersonic shock wave laminar boundary layer interactions is evaluated. SU2-NEMO, a recent enhancement to the open-source SU2 multi-physics suite, introduces improved capabilities for handling high-enthalpy and high-Mach number flows. Computations performed using SU2 are presented for a generic body (cylinder) and compared with experimental data. The results demonstrate the current strengths and limitations of modern CFD methods for these types of flows.

Keywords: SU2; nonequilibrium flows; high-temperature effects; aerothermodynamics; hypersonic flight; computational fluid dynamics;

[1] E-mail: celikene18@itu.edu.tr
Advisor: Prof.Dr.Bayram Çelik, Astronautical Engineering, Istanbul Technical University, celikbay.itu.edu.tr

II. Introduction and Objectives

Introduction

Despite ongoing research, simulating high-Mach flows is still a major challenge in computational fluid dynamics (CFD). From a design perspective, accurately predicting the aerothermodynamic environment, which is not in equilibrium, is crucial for developing and optimizing vehicle systems to withstand the large aerodynamic and thermal loads during hypersonic flight. This prediction is difficult due to the finite-rate processes caused by highly energetic molecular collisions, which impact both fluid bulk and transport properties. Creating efficient and reliable computational models that effectively capture the interaction between fluid motion, chemical reactions, and thermodynamic processes is still a key focus in CFD research.

High-temperature effects in the hypersonic regime are due to high-flow kinetic energy relative to the static thermal enthalpy. This situation can lead to finite-rate kinetic processes when the flow is rapidly decelerated, such as across a strong shock. When these processes have a relaxation time similar to the fluid's mechanical residence time, a state of thermochemical nonequilibrium is created. In this nonequilibrium state, the thermodynamic properties and species concentrations need to be detailed spatially to accurately model the flow. High fluid-specific energy densities make it challenging and costly to replicate the mission-relevant time and length scales, especially in ground-based experiments and during vehicle design analysis. As the flow enthalpy increases, nonequilibrium effects become more significant and complex, requiring additional models to accurately represent the underlying physics [1]. There are various numerical solvers developed to solve these problems.

The Langley Aerothermodynamic Upwind Relaxation Algorithm (LAURA) [2] is a computational fluid dynamics code designed for simulating viscous, hypersonic flow fields around aerospace vehicles, particularly those involving complex thermochemical nonequilibrium processes. Developed by NASA, LAURA employs an implicit numerical approach to solve the Navier-Stokes equations, facilitating accurate modeling of aerothermodynamic phenomena such as aeroassisted orbital transfer, scramjet propulsion, and single-stage-to-orbit vehicles. The algorithm uses structured grids, upwind schemes, and total variation diminishing methods to handle shocks and discontinuities, while its modular design allows for customization and efficient parallel processing [2]. Through detailed user manuals and comprehensive documentation, LAURA provides robust tools for researchers to simulate and analyze the aerodynamic and thermal performance of high-speed aerospace vehicles.

The Data-Parallel Line Relaxation (DPLR) [3] an advanced numerical technique designed for solving the Navier-Stokes equations on massively parallel supercomputers. It modifies the traditional Gauss-Seidel line relaxation method to suit parallel computing by replacing Gauss-Seidel sweeps with line relaxation steps, effectively removing data dependencies and enabling simultaneous parallel computation. The DPLR method demonstrates superior convergence properties, especially for high-Reynolds-number flows, by moving body-normal terms to the left-hand side and solving them as block tridiagonal systems. This approach significantly reduces computation time and enhances parallel efficiency, making it highly effective for large-scale viscous flow simulations on parallel architectures like the Cray T3E and Thinking Machines CM-5.[4]

The US3D code, developed by the University of Minnesota in collaboration with NASA Ames Research Center, is a sophisticated computational fluid dynamics (CFD) tool designed for simulating complex compressible and reacting flows [5]. It builds on the foundation of the well-known NASA DPLR code but introduces significant advancements through the use of unstructured grids, enhancing its flexibility for various flow problems. US3D is capable of handling a wide range of multi-physics scenarios including gas-phase kinetics, internal energy relaxation, gas-surface interactions, turbulence, and fluid-structure interactions. It employs advanced numerical methods, including high-order, low-dissipation flux functions and dynamic grid motion capabilities, making it particularly suitable for high-fidelity aerothermodynamics and hypersonic flow simulations [6]. The code's development focused on achieving production-level maturity, ensuring robustness, and enabling extensive parallel scalability for large-scale computations. There have also been several open-source codes developed for modeling flows in thermochemical nonequilibrium such as OpenFoam CFD framework, hy2Foam and COOLFLUID

hy2Foam [7] is an open-source two-temperature CFD solver developed at the University of Strathclyde, designed for simulating hypersonic reacting flows. It operates within the OpenFoam framework and has been validated for zero-dimensional test cases. The solver uses a combination of the coupled vibration-dissociation-vibration (CVDV) model and quantum-kinetic (QK) rates [8], offering a novel approach to modeling energy exchange processes. It aims to

provide students and researchers with access to state-of-the-art hypersonic CFD capabilities and serves as a foundation for future hybrid CFD-DSMC codes. In addition, COOLFluiD [9], developed at the Von Karman Institute for Fluid Dynamics and the KU Leuven Center for Mathematical Plasma Astrophysics, uses advanced numerical methods to solve multi-physics problems on unstructured grids. It has been applied to various fields, including re-entry aerothermodynamics, aeroacoustics, turbulence modeling, and plasma dynamics.

The SU2 [10] suite is an open-source computational analysis and design package designed to solve multiphysics analysis and optimization tasks using unstructured mesh topologies. Its architecture is unique in its extensibility, allowing it to treat a wide range of partial-differential-equation-based problems that were not initially envisioned. This adaptability enables the rapid implementation of new physics packages that can be tightly coupled to form a powerful ensemble of analysis tools. SU2's core is a Reynolds-averaged Navier–Stokes (RANS) solver capable of simulating compressible, turbulent flows. Additionally, through the use of an adjoint method, SU2 provides gradient information for optimal shape design, uncertainty quantification, and adaptive mesh refinement. This information allows for sophisticated analysis and design strategies for complex, multiphysics engineering systems.

The SU2-NEMO [11] library, is an extension of the SU2 multiphysics suite designed to simulate high-enthalpy and high-Mach number flows, particularly those involving thermal nonequilibrium and finite-rate chemistry. It integrates the Mutation++ physio-chemical library to enhance its modeling capabilities. The library's architecture is modular, allowing for the efficient addition of new models. SU2-NEMO employs advanced numerical formulations and discretization schemes for convective fluxes, and its performance has been validated through various two- and three-dimensional test cases. The framework facilitates the rapid implementation of new thermochemical models and numerical schemes, ensuring robust and accurate simulation of complex nonequilibrium flows essential for hypersonic vehicle design and analysis.

The software's development was driven by several core principles to ensure its utility and longevity. These principles include encouraging community involvement via an open-source model, promoting code reusability and encapsulation through high-level abstractions, ensuring portability and ease of use by relying on standard C++ and widely available open-source software, and focusing on performance for large-scale simulations through efficient algorithms for massively parallel architectures. SU2 is released under a nonviral open-source license, making it freely available for the community to use, verify, and contribute to. This open model supports the advancement of numerical methods and computational fluid dynamics, fostering a collaborative environment for researchers worldwide.

Objectives

Our main objectives is that validate using SU2 CFD software series of experiments conducted by the German Aerospace Center (DLR) to investigate hypersonic shock interactions, particularly focusing on the flow past cylindrical models. These experiments were performed in the high enthalpy shock tunnel (HEG) at different total enthalpies (HEG conditions I and III), using air as the test gas. The experimental setup included pressure transducers and thermocouples distributed along the cylinder to measure surface pressure and heat flux distributions. The data collected from these experiments provided valuable insights into non-equilibrium chemical relaxation processes and their impact on the density distribution and shock standoff distance, offering a robust basis for validating CFD simulations, such as those conducted using the SU2 software. The validation process involves comparing the CFD results with the detailed experimental measurements of surface pressure, heat flux, and other flow characteristics to assess the accuracy and reliability of the SU2 predictions under hypersonic flow conditions.

Experiment

A test campaign was conducted at the High Enthalpy Shock Tunnel (HEG) [12] of the German Aerospace Center (DLR) to investigate the flow past a cylindrical model. The cylindrical model, with a radius of 45 mm and a span of 380 mm, was mounted on the nozzle centerline with its axis perpendicular to the flow. It was equipped with 17 pressure transducers and an equal number of thermocouples to measure surface pressure and heat flux distributions. These transducers were arranged along six rows near the plane of symmetry at the mid-span, positioned 10, 20, and 30 mm to the left and right of the plane of symmetry, covering a circumferential angle of minus 60 degree and plus 60 degree with respect to the inflow direction.

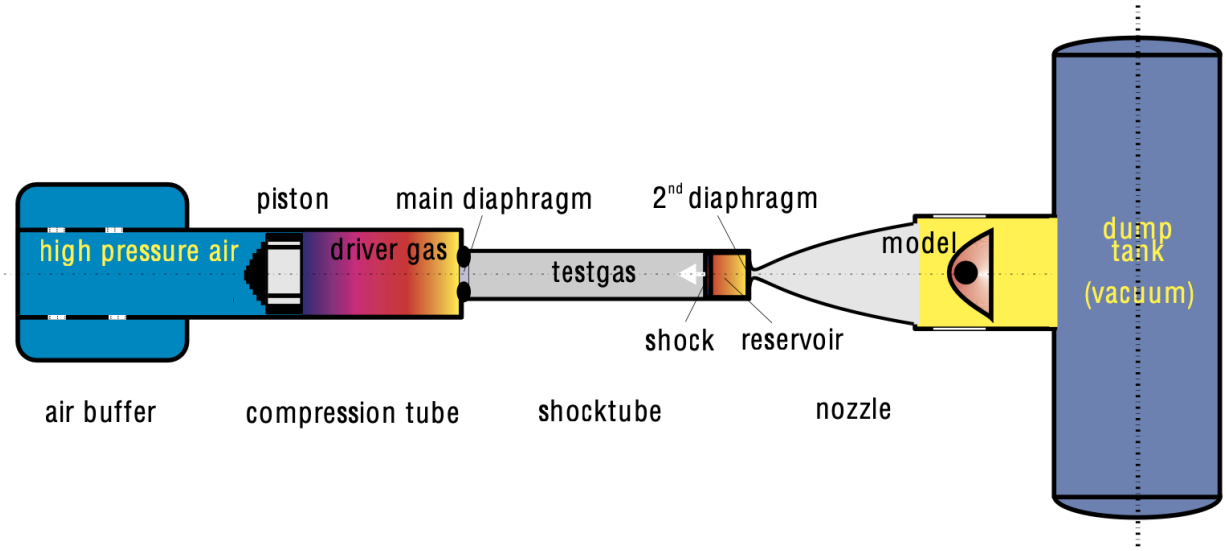

Figure 1 Schematic of the HEG

The large shock standoff distance of this setup allowed the use of optical measurement techniques to determine the gas properties in the shock layer. Holographic interferometry and time-resolved Schlieren were used to measure density distributions in the shock layer and the temporal evolution of the bow shock shape. Freestream static and pitot pressures, along with stagnation heat transfer on a sphere, were recorded during each run for calibration, normalization, and statistical analysis.

Measurements on the cylinder were performed at different total enthalpies (HEG conditions I and III, 22.4 MJ/kg and 13.5 MJ/kg, respectively) using air as the test gas. The HEG reservoir and freestream data for these measurements are listed in Table 2. Under the experimental conditions, the flow in the shock layer is subject to nonequilibrium chemical relaxation processes that significantly affect the density distribution and shock standoff distance [13].

Quantity	I	III
H_o (MJ/kg)	22.4	13.5
p_o (MPa)	35.0	48.3
T_o (K)	9200	7370
U_∞ (m/s)	5956	4776
p_∞ (Pa)	476	687
ρ_∞ (kg/m^3)	1.547×10^{-3}	3.26×10^{-3}
T_∞ (K)	901	694
p_{p_∞} (kPa)	52.9	70.8
M_∞	8.98	8.78
$Y[N_2]_\infty$	0.7543	0.7356
$Y[O_2]_\infty$	0.00713	0.1340
$Y[NO]_\infty$	0.01026	0.0509
$Y[N]_\infty$	6.5×10^{-7}	0.0000
$Y[O]_\infty$	0.2283	0.07955

Figure 2 Test condition for cylinder

III.Methods and Resources

Methods Used in This Project

Meshing Using Custom Fortran Code

In our project, we employed a custom Fortran code to generate structured cylindrical mesh specifically for conducting CFD (Computational Fluid Dynamics) analyses on 2D cylindrical bodies at high Mach numbers (above Mach 8). The code was designed to meticulously construct grids and compute exact solutions for various cylinder shapes, including the Karman-Trefftz cylinder, which encompasses the Jukowsky cylinder as a special case.

The methodology involved generating boundary points of the cylinder and Cp distribution, which were then used as inputs for other grid generation programs. Structured grids over the domain were created, and exact solutions were computed on these grid points to validate the flow simulations. This was crucial for analyzing the behavior of airflow over the cylindrical body under high-speed conditions.

The code version we used allowed for detailed adjustments such as the angle of attack, thickness, camber, and trailing edge angle, which are critical in simulating realistic aerospace conditions. This approach not only supported our analysis of high-temperature non-equilibrium effects on the cylindrical body but also enhanced the accuracy of our computational models by providing a robust framework for simulating complex aerodynamic phenomena.

Computational Fluid Dynamics (CFD) Simulations

To implement the cylindrical mesh created by our custom Fortran code into the SU2 solver for continuum flow analysis, the process involves several key steps. Here's a breakdown of how this integration can be conducted effectively:

Mesh Generation and Export:

- Using the custom Fortran code, generate a structured cylindrical mesh tailored to the specific requirements of the 2D cylindrical body analysis. This mesh must account for the aerodynamic and thermal considerations relevant to lower altitude reentry scenarios.
- Ensure the mesh has appropriate resolution and boundary definitions to accurately represent the physical geometry and expected flow conditions.
- Export this mesh in a format compatible with SU2, such as the `.su2` format, which includes necessary information on nodes, elements, and boundary conditions.

Preparation for SU2:

- Convert or confirm the mesh file is in the `.su2` format, ensuring it includes all boundary conditions and node information required by SU2 for effective simulations.
- Define the physical and simulation parameters in SU2's configuration file. These parameters include fluid properties, operating conditions (like altitude and velocity), and solver settings tailored to simulate continuum flow dynamics using the Navier-Stokes equations.
- Set up boundary conditions in SU2 to match the experimental setup, focusing on ensuring that the inflow and outflow conditions accurately reflect the reentry scenario being modeled.

SU2 Simulation Execution:

- Load the cylindrical mesh and configuration files into SU2.
- Run the simulation, allowing SU2 to apply its continuum-based Navier-Stokes solvers to calculate aerodynamic forces and heat transfer characteristics under the specified reentry conditions.
- Monitor the simulation to ensure stability and accuracy, adjusting mesh density or solver settings as needed based on preliminary results or convergence behavior.

Data Analysis and Validation:

- Analyze the output data from SU2, focusing on parameters like pressure distributions, temperature fields, and flow velocities around the cylindrical body.
- Compare these results with theoretical predictions and experimental data to validate the simulation's accuracy.
- Use the insights gained to refine the mesh or simulation parameters for subsequent simulations to enhance accuracy and reliability.

Integration with SPARTA for High-Altitude Analysis:

-For high-altitude scenarios where gas becomes rarefied, employ SPARTA using the DSMC method. This step might involve adjusting the mesh or using a different set of boundary and initial conditions suitable for DSMC simulations.

- Ensure that both SU2 and SPARTA simulations use consistent geometrical and operational parameters to allow comparative analysis between continuum and rarefied flow conditions.

By following these steps, the cylindrical mesh generated by the custom Fortran code can be effectively utilized in SU2 to simulate lower altitude reentry scenarios, providing detailed insights into the aerodynamics and thermal dynamics experienced by the vehicle. This integrated approach enables a comprehensive analysis of reentry dynamics across different atmospheric densities.

Data Analysis and Comparative Study

After completing the simulations with SU2 and SPARTA, we process and analyze the data using Paraview. This analysis allows us to closely examine the aerodynamic and thermal characteristics of reentry vehicles under various conditions. By studying these characteristics, we gain valuable insights into the performance and resilience of the vehicles during reentry.

A key part of our methodology is the comparative analysis between the results from SU2 and SPARTA. We compare these results to evaluate the applicability, accuracy, and computational efficiency of each simulation method across different atmospheric conditions. This comparison is particularly focused on the transition from continuum to rarefied conditions. Our goal is to identify the strengths and weaknesses of each approach, which will help guide the selection of methods for future studies in this area.

Analysis of The Resources for This Project

Human Resources

This research project is executed by a dedicated team of two undergraduate students at Istanbul Technical University, under the mentorship and guidance of experienced faculty advisors. The team's responsibilities are judiciously divided to ensure efficiency and thoroughness. Key responsibilities include:

Conducting Simulations: Operating and monitoring the CFD simulations using both SU2 and SPARTA, adjusting parameters as necessary to explore various reentry scenarios.
Data Analysis: Carefully analyzing the data obtained from the simulations to extract meaningful insights about the aerodynamic and thermal behaviors of the reentry vehicles.
Report Preparation: Compiling the findings, analyses, and methodologies into a comprehensive final report, ensuring clear communication of the research outcomes.

Technical Resources

High-Performance Computing: Access to high-performance computing facilities is provided by Istanbul Technical University. These facilities, encompassing advanced processors and ample memory, are critical for handling the intensive computational demands of CFD simulations. The availability of such resources is vital for the success of our simulations, particularly for the processor-intensive DSMC simulations conducted in SPARTA.
Software Accessibility: Both SU2 and SPARTA are accessed through open-source platforms. This not only ensures cost-effective utilization of these advanced simulation tools but also promotes transparency and reproducibility in our research methodologies.

Time Allocation and Management

Processor Time and Simulation Runs: Due to the extensive computational requirements, particularly for the DSMC simulations, we have allocated substantial processor time. Simulations are strategically scheduled during off-peak hours to optimize resource usage and efficiency.
Project Timeline: The project is meticulously planned over a predetermined duration, with specific milestones set for simulation setup, data collection, analysis, and report drafting. A detailed timeline, included in the appendix of our report, outlines the schedule and key phases of the project, ensuring systematic progress and timely completion.

Additional Resources

Documentation and Data Visualization: Resources allocated for documentation include software tools for data analysis and graphical representation, enabling us to effectively visualize and interpret complex datasets.
Report Compilation: The final stage involves utilizing document preparation software to compile our findings and analyses into a well-structured and accessible report, an essential component for communicating our research to the academic community and other interested parties.

IV. Section(s) Specific to The Graduation Project

Thermochemical Nonequilibrium Navier-Stokes Equations

Navier-Stokes Equations: These are fundamental in fluid dynamics and describe the motion of fluid substances. They express the conservation of mass (continuity), momentum, and energy in fluid flow.

Thermochemical Nonequilibrium: In the context of atmospheric reentry, the air around the spacecraft is not only moving at high speeds but is also subjected to extremely high temperatures, leading to chemical reactions and changes in the thermal state of the gas. Thermochemical nonequilibrium refers to the state where different parts of the gas mixture (like atomic oxygen, nitrogen, etc.) may have different temperatures (translational, rotational, vibrational, and electronic). This means the chemical composition and the energy state of the gas are constantly changing.

Application in Reentry Analysis: For reentry vehicles, understanding the behavior of the shock layer that forms in front of the vehicle is crucial. Under these extreme conditions, the assumption of a chemically and thermally equilibrium gas (as in standard Navier-Stokes equations) is no longer valid. The Thermochemical Nonequilibrium Navier-Stokes equations modify the standard equations to account for these nonequilibrium effects, allowing for a more accurate simulation of the flow field and heat transfer around the reentry vehicle.

Two Temperature Model

The two-temperature model is a widely used approach in computational fluid dynamics (CFD) to simulate hypersonic nonequilibrium flows, where the flow involves complex physical and chemical processes such as vibrational and electronic energy excitation, molecular dissociation, and ionization. This model distinguishes between the translational-rotational temperature (T) and the vibrational-electronic temperature (Tv), recognizing that these modes of energy can be at different levels of excitation in nonequilibrium conditions. The model assumes that each internal energy mode follows a Boltzmann distribution corresponding to its temperature, allowing for separate treatment of thermal and chemical nonequilibrium effects. Despite its empirical nature and limitations, such as reliance on outdated reaction rate data and assumptions of equilibrium within each mode, the two-temperature model has been integrated into many CFD codes for practical engineering applications. Recent advancements aim to enhance its accuracy by incorporating corrections based on high-fidelity state-to-state (StS) models and quasi-classical trajectory (QCT) derived data.

Gupta-Yos Transport Model

Transport Phenomena: This refers to the study of momentum, energy, and mass transfer in fluids. In high-speed aerodynamics, especially under nonequilibrium conditions, understanding how these quantities are transported is crucial.

Gupta-Yos Model: Developed by Gupta and Yos, this model provides a method to calculate the transport properties (like viscosity, thermal conductivity, and diffusion coefficients) of air in high-temperature conditions, typical of reentry scenarios. The model is particularly tailored for air mixtures at high temperatures, where traditional transport models may not be accurate.

Integration with Navier-Stokes: The Gupta-Yos model is often used in conjunction with the Thermochemical Nonequilibrium Navier-Stokes equations. While the Navier-Stokes equations govern the overall fluid flow, the Gupta-Yos model provides the necessary transport property data, which are critical for accurately solving these equations under nonequilibrium conditions.

Governing Equations

Thermochemical Nonequilibrium Navier-Stokes

The equation that given below is a general form of the Navier-Stokes equations used in computational fluid dynamics (CFD). It represents the conservation laws of fluid dynamics, including continuity, momentum, and energy equations. Here is the detailed explanation of each term:

$$\mathbf{R}(\mathbf{U}, \nabla\mathbf{U}) = \frac{\partial \mathbf{U}}{\partial t} + \nabla \cdot \mathbf{F}^c(\mathbf{U}) - \nabla \cdot \mathbf{F}^v(\mathbf{U}, \nabla\mathbf{U}) - \mathbf{Q}(\mathbf{U}) = 0 \tag{1}$$

$\mathbf{R}(\mathbf{U}, \nabla\mathbf{U})$: Residual term

$\mathbf{U}$: Vector of conservative variables (e.g., density, momentum, energy)

$\frac{\partial \mathbf{U}}{\partial t}$: Temporal change of the conservative variables

$\nabla \cdot \mathbf{F}^c(\mathbf{U})$: Divergence of the convective fluxes

$\mathbf{F}^c(\mathbf{U})$: Convective flux vector

$\nabla \cdot \mathbf{F}^v(\mathbf{U}, \nabla\mathbf{U})$: Divergence of the viscous fluxes

$\mathbf{F}^v(\mathbf{U}, \nabla\mathbf{U})$: Viscous flux vector

$\mathbf{Q}(\mathbf{U})$: Source term (e.g., external forces, reactions)

Conserved variables in the context of fluid dynamics and the Navier-Stokes equations are quantities that remain constant in a closed system despite the internal interactions and processes occurring within the fluid. These variables are typically derived from fundamental conservation laws, such as the conservation of mass, momentum, and energy. In the context of multi-species, compressible fluid flow, the conserved variables often include:

$$\mathbf{U} = \begin{pmatrix} \rho_1 \\ \vdots \\ \rho_{ns} \\ \rho\mathbf{u} \\ \rho e \\ \rho e^{ve} \end{pmatrix}$$

$\mathbf{U}$: Vector of conserved variables
ρ_i : Density of species i
ns : Number of species
ρ : Total density
$\mathbf{u}$: Velocity vector
e : Total energy
e^{ve} : Vibrational energy

Convective fluxes in fluid dynamics describe the transport of physical quantities such as mass, momentum, and energy due to the bulk motion of the fluid. These fluxes are a key component of the Navier-Stokes equations and represent the movement of conserved quantities as the fluid flows. Convective fluxes are contrasted with diffusive fluxes, which describe transport due to molecular diffusion or viscosity.

$$\mathbf{F}^c = \begin{pmatrix} \rho_1 \mathbf{u} \\ \vdots \\ \rho_{ns} \mathbf{u} \\ \rho \mathbf{u}\mathbf{u}^T + p\mathbf{I} \\ \rho h \mathbf{u} \\ \rho e^{ve} \mathbf{u} \end{pmatrix}$$

$\mathbf{F}^c$	Convective flux vector
ρ_i	Density of species i
ns	Number of species
$\mathbf{u}$	Velocity vector
ρ	Total density
p	Pressure
$\mathbf{I}$	Identity matrix
h	Total enthalpy
e^{ve}	Vibrational energy

Viscous fluxes in fluid dynamics represent the transport of physical quantities such as mass, momentum, and energy due to the internal friction within the fluid, which is associated with viscosity and molecular diffusion. Unlike convective fluxes, which are driven by the bulk motion of the fluid, viscous fluxes are driven by gradients in velocity, temperature, and concentration. These fluxes are essential in describing the diffusive transport phenomena in the fluid.

$$\mathbf{F}^v = \begin{pmatrix} -\mathbf{J}_1 \\ \vdots \\ -\mathbf{J}_{ns} \\ \mathbf{u}^T \sigma - \sum_k \mathbf{q}^k - \sum_s \mathbf{J}_s h_s \\ \sigma \\ -q^{ve} - \sum_s \mathbf{J}_s e^{ve} \end{pmatrix}$$

$\mathbf{F}^v$	Viscous flux vector
$\mathbf{J}_i$	Diffusive flux of species i
ns	Number of species
$\mathbf{u}$	Velocity vector
σ	Stress tensor
$\mathbf{q}^k$	Heat flux vector
h_s	Enthalpy of species s
q^{ve}	Vibrational energy flux
e^{ve}	Vibrational energy

In fluid dynamics, source terms represent external influences or internal processes that add or remove quantities such as mass, momentum, or energy from the system. They are crucial in accounting for phenomena that cannot be captured solely by convective and diffusive fluxes. Source terms are included in the governing equations to ensure the accurate representation of various physical processes within the fluid.

$$\mathbf{Q} = \begin{pmatrix} \omega_1 \\ \vdots \\ \omega_{ns} \\ 0 \\ 0 \\ \dot{H}^{tr:ve} + \sum_s \omega_s e^{ve} \end{pmatrix}$$

$\mathbf{Q}$	Source terms vector
ω_i	Source term for species i
ns	Number of species
$\dot{H}^{tr:ve}$	Energy transfer rate
e^{ve}	Vibrational energy

The notation in the previously mentioned equations largely mirrors that used in the compressible Navier-Stokes equations. A separate mass conservation equation is established for each chemical species, denoted by s within the range of 1 to n_s. Each of these equations includes a source term, ω_s, representing the volume-specific production rate of species s due to chemical reactions within the flow. The chemical production rates are calculated as:

$$\dot{w}_s = M_s \sum_r (\beta_{s,r} - \alpha_{s,r})(R_r^f - R_r^b)$$

Two Temperature Model

SU2-NEMO (Nonequilibrium Multi-physics) is a specialized module within the SU2 suite of CFD tools designed to handle such nonequilibrium flow simulations. It implements the two-temperature model, solving coupled Navier-Stokes and energy equations for T_{tr} and T_{ve} to capture the complex interactions between different energy modes. SU2-NEMO incorporates detailed chemical kinetics and thermodynamic models to simulate high-temperature effects such as dissociation and ionization, validated against experimental data and high-fidelity state-to-state simulations. This module is crucial for aerospace applications, enabling accurate predictions of flow properties and improving the design and safety of hypersonic vehicles and reentry capsules by reflecting the true behavior of gases under extreme conditions.

The two-temperature model [14] is an essential approach for capturing the nonequilibrium conditions in hypersonic flows, where translational-rotational and vibrational-electronic energy modes do not equilibrate at the same rate. This model separates the temperatures for these energy modes, using T_{tr} for translational-rotational and T_{ve} for vibrational-electronic modes. Translational and rotational energies are assumed to be in equilibrium and modeled using rigid body dynamics, while vibrational energy is approximated with a harmonic oscillator model. This separation allows the model to accurately reflect the different rates at which these energy modes reach equilibrium, providing a more precise representation of the physical processes occurring in high-temperature, nonequilibrium environments.Through the independence of the energy levels, the total energy and vibrational– electronic energy per unit volume can be expressed as

$$\rho e = \sum_s \rho_s \left(e_s^{tr} + e_s^{rot} + e_s^{vib} + e_s^{el} + e_s^{\circ} \right) + \frac{1}{2} \mathbf{u}^T \mathbf{u}$$

ρ	Total density
e	Total energy per unit mass
ρ_s	Density of species s
e_s^{tr}	Translational energy per unit mass for species s
e_s^{rot}	Rotational energy per unit mass for species s
e_s^{vib}	Vibrational energy per unit mass for species s
e_s^{el}	Electronic energy per unit mass for species s
e_s°	Chemical energy per unit mass for species s
$\mathbf{u}$	Velocity vector
$\frac{1}{2}\mathbf{u}^T\mathbf{u}$	Kinetic energy per unit mass

$$\rho e^{ve} = \sum_s \rho_s \left(e_s^{vib} + e_s^{el}\right)$$

ρ	Total density
e^{ve}	Vibrational and electronic energy per unit mass
ρ_s	Density of species s
e_s^{vib}	Vibrational energy per unit mass for species s
e_s^{el}	Electronic energy per unit mass for species s

Considering a general gas mixture consisting of polyatomic, monatomic, and free electron species, expressions for the energy stored in the translational, rotational, vibrational, and electronic modes are given as

$$e_s^{tr} = \begin{cases} \frac{3}{2}\frac{R}{M_s}T & \text{for monatomic and polyatomic species,} \\ 0 & \text{for electrons,} \end{cases}$$

$$e_s^{rot} = \begin{cases} \frac{\xi}{2}\frac{R}{M_s}T & \text{for polyatomic species,} \\ 0 & \text{for monatomic species and electrons,} \end{cases}$$

$$e_s^{vib} = \begin{cases} \frac{R}{M_s}\frac{\theta_s^{vib}}{exp\left(\theta_s^{vib}/T^{ve}\right)-1} & \text{for polyatomic species,} \\ 0 & \text{for monatomic species and electrons,} \end{cases}$$

$$e_s^{el} = \begin{cases} \frac{R}{M_s}\frac{\sum_{i=1}^{\infty} g_{i,s}\theta_{i,s}^{el} exp(-\theta_{i,s}^{el}/T_{ve})}{\sum_{i=0}^{\infty} g_{i,s} exp(-\theta_{i,s}^{el}/T_{ve})} & \text{for polyatomic and monatomic species,} \\ \frac{3}{2}\frac{R}{M_s}T^{ve} & \text{for electrons,} \end{cases}$$

Gupta-Yos Transport Model

The created by Gupta emphasizes the transport characteristics of weakly ionized flows. It tends to be more precise than the Wilkes-Blottner-Eucken model when dealing with temperatures exceeding 10,000 K. The formulas determining the transport coefficients in this model are reliant on the terms related to collisions.

$$\Delta_{s,r}^{(1)}(T) = \frac{8}{3}\left[\frac{2M_sM_r}{\pi RT(M_s+M_r)}\right]^{1/2}\pi\Omega_{s,r}^{(1,1)}$$

$$\Delta_{s,r}^{(2)}(T) = \frac{16}{5}\left[\frac{2M_sM_r}{\pi RT(M_s+M_r)}\right]^{1/2}\pi\Omega_{s,r}^{(2,2)}$$

The computation of collision cross-sections in this model follows the approach outlined in the Wilkes-Blottner-Eucken section. The viscosity of the mixture is determined using a specific formula.

$$\mu = \sum_{s\neq e}\frac{m_s\gamma_s}{\sum_{r\neq e}\gamma_r\Delta_{s,r}^{(2)}(T_{tr}) + \gamma_r\Delta_{e,r}^{(2)}(T_{ve})} + \frac{m_e\gamma_e}{\sum_r \gamma_r\Delta_{e,r}^{(2)}(T_{ve})}$$

where

$$\gamma_s = \frac{\rho_s}{\rho M_s}.$$

The calculation of thermal conductivity considers various energy modes. Specifically, the contribution from translational modes is formulated as follows.

$$\kappa_t = \frac{15}{4}k_B\sum_{s\neq e}\frac{\gamma_s}{\sum_{r\neq e}a_{s,r}\gamma_r\Delta_{s,r}^{(2)}(T_{tr}) + 3.54\gamma_e\Delta_{s,e}^{(2)}(T_{ve})},$$

and where

$$a_{s,r} = 1 + \frac{\left[1 - (m_s/m_r)\right]\left[0.45 - 2.54(m_s/m_r)\right]}{\left[1 + (m_s/m_r)\right]^2}$$

And where

$$m_s = \frac{M_s}{N_{av}}$$

In this context, Nav represents Avogadro's Number. The thermal conductivity related to the rotational modes is described using a different expression.

$$\kappa_r = k_B \sum_{s \neq e} \frac{\gamma_s}{\sum_{r \neq e} \gamma_r \Delta^{(1)}_{s,r}(T_{tr}) + \gamma_e \Delta^{(1)}_{s,e}(T_{ve})}.$$

The combined thermal conductivity for translational and rotational modes in the mixture can subsequently be articulated using a specific formula.

$$\kappa_{tr} = \kappa_t + \kappa_r.$$

The vibrational/electronic mode thermal conductivity is

$$\kappa_{ve} = k_B \frac{C_{ve}}{R} \sum_{s \in molecules} \frac{\gamma_s}{\sum_{r \neq e} \gamma_r \Delta^{(1)}_{s,r}(T_{tr}) + \gamma_e \Delta^{(1)}_{s,r}(T_{ve})}$$

and the thermal conductivity for electrons is given by

$$\kappa_e = \frac{15}{4} k_B \frac{\gamma_e}{\sum_r 1.45 \gamma_r \Delta^{(2)}_{e,r}(T_{ve})}.$$

Finally, the binary diffusion coefficient for heavy particles is given by

$$D_{s,r} = \frac{k_B T_{tr}}{p \Delta^{(1)}_{s,r}(T_{tr})},$$

and for electrons

$$D_{e,r} = \frac{k_B T_{ve}}{p \Delta^{(1)}_{e,r}(T_{ve})}.$$

Reaction	C_r ((cm^3)/(mol-s))	η_r	$epsilon_r^A$ (K)
$N_2 + e^- \rightleftharpoons N + N + e^-$	3.0×10^{24}	−1.6	113,200
$N_2 + N_2 \rightleftharpoons 2N + O_2$	7.0×10^{21}	−1.60	113,200
$N_2 + O_2 \rightleftharpoons 2N + O_2$	7.0×10^{21}	−1.60	113,200
$N_2 + NO \rightleftharpoons 2N + NO$	7.0×10^{21}	−1.60	113,200
$N_2 + N \rightleftharpoons 2N + NO$	3.0×10^{22}	−1.60	113,200
$N_2 + O \rightleftharpoons 2N + NO$	3.0×10^{22}	−1.60	113,200
$O_2 + N_2 \rightleftharpoons 2O + N_2$	2.0×10^{21}	−1.50	59,500
$O_2 + O_2 \rightleftharpoons 2O + O_2$	2.0×10^{21}	−1.50	59,500
$O_2 + NO \rightleftharpoons 2O + NO$	2.0×10^{21}	−1.50	59,500
$O_2 + N \rightleftharpoons 2O + N$	1.0×10^{22}	−1.50	595,200
$O_2 + O \rightleftharpoons 2O + O$	1.0×10^{22}	−1.50	595,200
$NO + N_2 \rightleftharpoons N + O + N_2$	5.0×10^{15}	0.00	75,500
$NO + O_2 \rightleftharpoons N + O + O_2$	5.0×10^{15}	0.00	75,500
$NO + NO \rightleftharpoons N + O + NO$	5.0×10^{15}	0.00	75,500

Table 1 Arrhenius parameters for forward rate reactions.

Reaction	a_r^f	b_r^f	a_r^b	b_r^b
$N_2 + M \rightleftharpoons 2N + O_2$	0.5	0.5	1.0	0.0
$N_2 + M \rightleftharpoons 2O + O_2$	0.5	0.5	1.0	0.0
$NO + M \rightleftharpoons N + O + NO$	0.5	0.5	1.0	0.0
$N_2 + O \rightleftharpoons NO + N$	1.0	0.0	1.0	0.0
$NO + O \rightleftharpoons O_2 + N$	1.0	0.0	1.0	0.0
$N + O \rightleftharpoons NO^+ + e^-$	1.0	0.0	1.0	0.0

Table 2 Reaction rate coefficient controlling temperature factors.

Reaction	N (1/cm^3)	A_0	A_1	A_2	A_3	A_4
$N_2 + M \rightleftharpoons 2N + M$	1×10^{14}	3.4907	0.83133	4.0978	−12.728	0.7487
	1×10^{15}	2.0723	1.38970	2.0617	−11.828	0.015105
	1×10^{16}	1.6060	1.57320	1.3923	−11.533	−0.004543
	1×10^{17}	1.5351	1.60610	1.2993	−11.494	−0.00698
	1×10^{18}	1.4766	1.62910	1.2153	−11.457	−0.00944
	1×10^{19}	1.4766	1.62910	1.2153	−11.457	−0.00944
$O_2 + M \rightleftharpoons 2O + M$	1×10^{14}	1.8103	1.9607	3.5716	−7.3623	0.083861
	1×10^{15}	0.91354	2.3160	2.2885	−6.7969	0.046338
	1×10^{16}	0.64183	2.4253	1.9026	−6.6277	0.035151
	1×10^{17}	0.55388	2.4600	1.7763	−6.5720	0.031445
	1×10^{18}	0.52455	2.4715	1.7342	−6.55534	0.030209
	1×10^{19}	0.50989	2.4773	1.7132	−6.5441	0.29591
$NO + M \rightleftharpoons N + O + M$	1×10^{14}	2.1649	0.078577	2.8508	−8.5422	0.053043
	1×10^{15}	1.0072	0.53545	1.1911	−7.8098	0.004394
	1×10^{16}	0.63817	0.68189	0.66336	−7.5773	−0.011025
	1×10^{17}	0.55889	0.71558	0.55396	−7.5304	−0.014089
	1×10^{18}	0.5150	0.73286	0.49096	−7.5025	−0.015938
	1×10^{19}	0.50765	0.73575	0.48042	−7.4979	−0.016247
$N_2 + O \rightleftharpoons N + O + M$	1×10^{14}	1.3261	0.75268	1.2474	−4.1857	0.02184
	1×10^{15}	1.0653	0.85417	0.87093	−4.0188	0.010721
	1×10^{16}	0.96794	0.89131	0.7291	−3.9555	0.006488
	1×10^{17}	0.97646	0.89043	0.74572	−3.9642	0.007123
	1×10^{18}	0.96188	0.89617	0.72479	−3.955	0.006509
	1×10^{19}	0.96921	0.89329	0.73531	−3.9596	0.006818
$NO + O \rightleftharpoons O_2 + N$	1×10^{14}	0.35438	−1.8821	−0.72111	−1.1797	−0.30831
	1×10^{15}	0.093613	−1.7806	−1.0975	−1.0128	−0.41949
	1×10^{16}	−0.003732	−1.7434	−1.2394	−0.94952	−0.046182
	1×10^{17}	0.004815	−1.7443	−1.2227	−0.95824	−0.45545
	1×10^{18}	−0.009758	−1.7386	−1.2436	−0.949	−0.046159
	1×10^{19}	−0.002428	−1.7415	−1.2331	−0.95365	−0.04585

Table 3 Parameters for the Park 1990 equilibrium reaction constants

Computatinal mesh and Boundary Conditions

Used Fortran program that used for creating mesh is designed to generate computational grids and compute exact solutions for the Karman-Trefftz (KT) cylinder, which includes the Jukowsky cylinder as a special case. It aims to assist in creating accurate grids and solutions for CFD (Computational Fluid Dynamics) applications, particularly for validating CFD codes and performing aerodynamic analyses. The program begins by defining essential constants and cylinder parameters such as chord length, angle of attack, thickness, camber, and trailing edge angle. It generates boundary points for the cylinder, computes the pressure coefficient distribution, and then creates structured quadrilateral and triangular grids over the computational domain. These grids are stored in various formats compatible with visualization and solver tools like Tecplot and SU2. The code also includes subroutines for writing these grids to files and performing exact solution computations at grid points. Radius of cylinder is 4.5 cm and distance from wall to farfield is 4cm.

The computational domain generated by this code is tailored for simulating thermochemical nonequilibrium flow using SU2, a popular open-source CFD software. The domain encompasses a KT cylinder, with the grid extending radially outward to a specified distance. The grid is designed to be structured, meaning it has a regular, predictable arrangement of grid points, which is crucial for ensuring numerical stability and accuracy in simulations. The domain includes both quadrilateral and triangular elements to offer flexibility in mesh refinement and computational efficiency. The outer boundary conditions are set to simulate far-field conditions, while the inner boundary conforms to the cylinder's shape. This setup allows for accurate simulation of flow characteristics around the cylinder, capturing critical details such as shock waves, boundary layers, and potential flow separation. By generating boundary data and exact solutions, the code facilitates detailed analysis and validation of the flow solver's performance under thermochemical nonequilibrium conditions. Diameter of cylinder is 4.5 cm and distance from wall to farfield is 4cm.

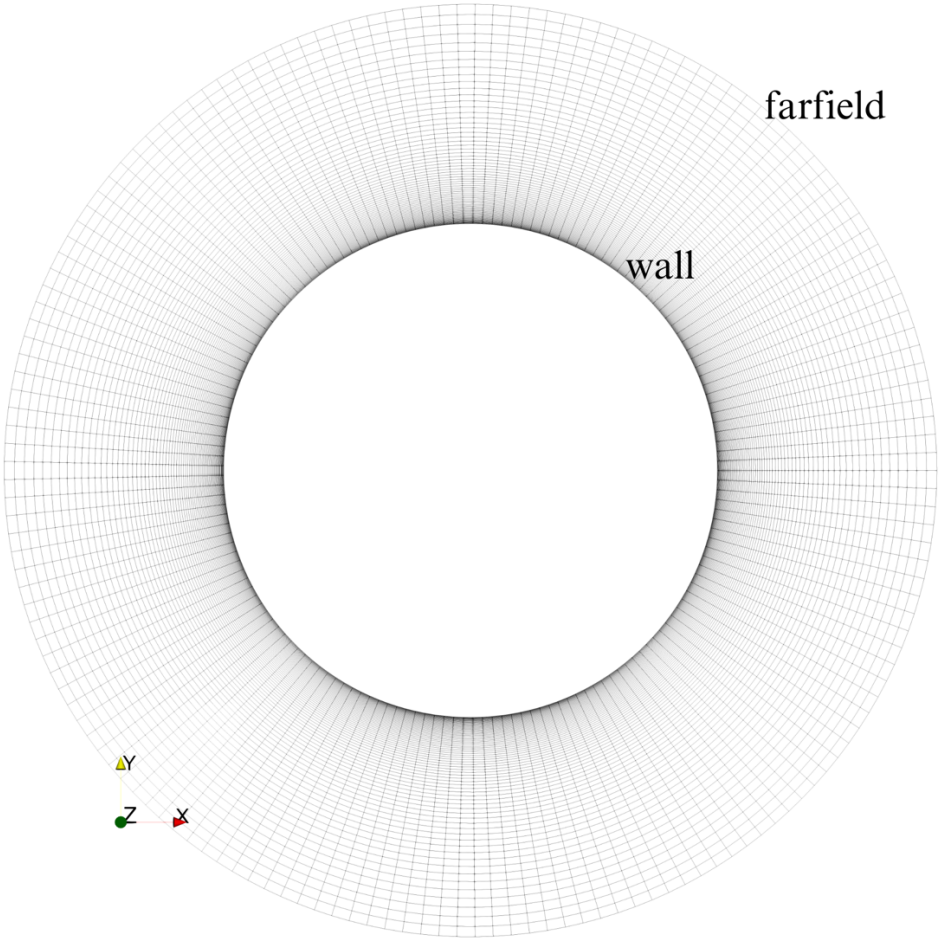

Figure 3 Computational Domain

V. Results and Conclusion

Results

In this study, we conducted a detailed numerical analysis of the pressure and heat flux distributions around a circular geometry using computational fluid dynamics (CFD) simulations. The results are summarized in the following observations:

Pressure Distribution

- The first image (Figure 4) shows the pressure distribution around the circular geometry. The color map indicates that the highest pressure region is located at the stagnation point, where the flow impinges directly on the surface. The pressure gradually decreases away from this point.
- The plot in the third image (Figure 6) quantitatively experimental data of the pressure values (black squares) along the surface of the circular geometry with the computed pressure (red line). The peak pressure value reaches approximately 58,000 Pa near the stagnation point, while lower pressure values are observed along the sides.

Heat Flux Distribution

- The second image (Figure 5) illustrates the heat flux distribution around the same circular geometry. Similar to the pressure distribution, the highest heat flux values are observed at the stagnation point, indicating intense thermal loading due to the high-speed flow.
- The fourth image (Figure 7) provides a detailed comparison of the heat flux (red line) and experimental data (black squares) along the surface. The peak heat flux reaches approximately 7.0e6 W/m^2 at the stagnation point, correlating well with the highest pressure region.

Conclusion

The numerical results obtained from the CFD simulations provide significant insights into the pressure and heat flux distributions around a circular geometry under high-speed flow conditions. The following conclusions can be drawn from the study:

Stagnation Point Dominance

- Both pressure and heat flux distributions exhibit maximum values at the stagnation point, where the fluid flow directly impacts the surface. This confirms the expected behavior in high-speed aerodynamic applications, where the stagnation region experiences the highest thermal and pressure loads.

Correlation Between Pressure and Heat Flux

- The comparison plots reveal a strong correlation between the pressure and heat flux distributions. The regions of high pressure correspond to high heat flux values, indicating that areas experiencing higher mechanical loads also undergo significant thermal stresses.

Validation with Experimental Data

- The numerical results show a good agreement with experimental data obtained from the German Aerospace Center (DLR) study. The pressure and heat flux values align closely with the experimental measurements, validating the accuracy of the CFD simulations performed using the SU2 software.

Implications for Design and Optimization

- The findings underscore the importance of accurately predicting pressure and heat flux distributions in the design and optimization of aerodynamic surfaces. Understanding these distributions helps in enhancing the thermal protection systems and structural integrity of high-speed vehicles

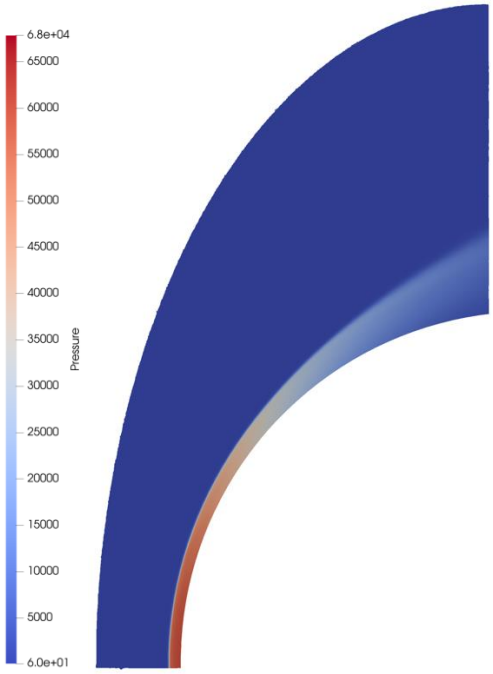

Figure 4 Pressure Distribution

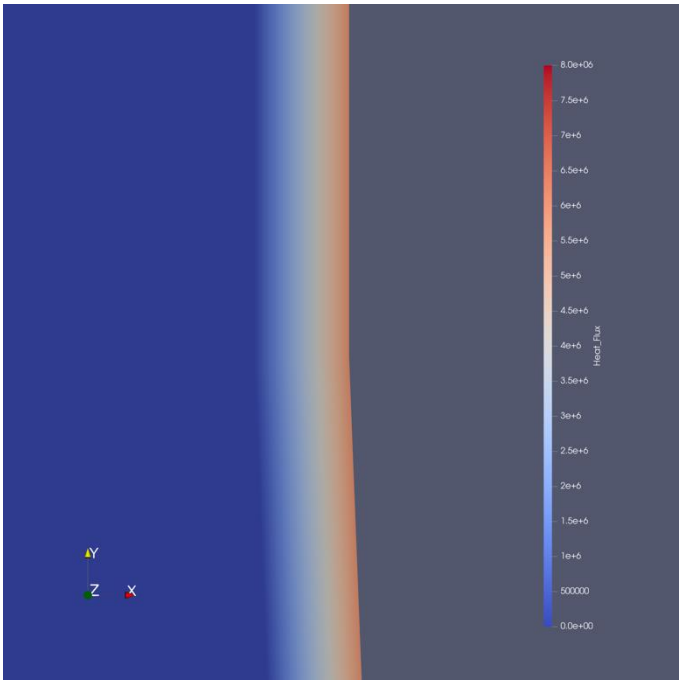

Figure 5 Heat Flux Distribution

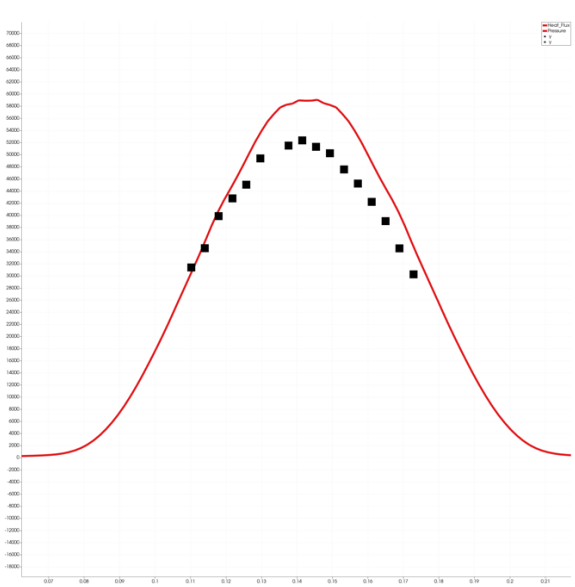

Figure 6 Comparison with experimental data pressure

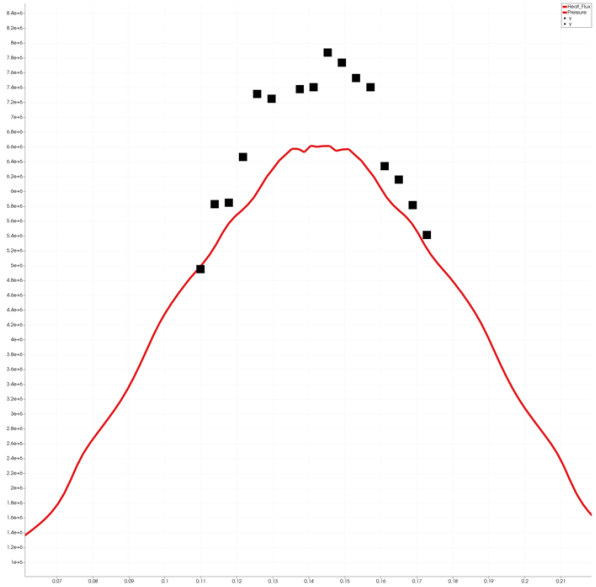

Figure 7 Comparison with experimental data heat flux

Appendices

A. Project Schedule

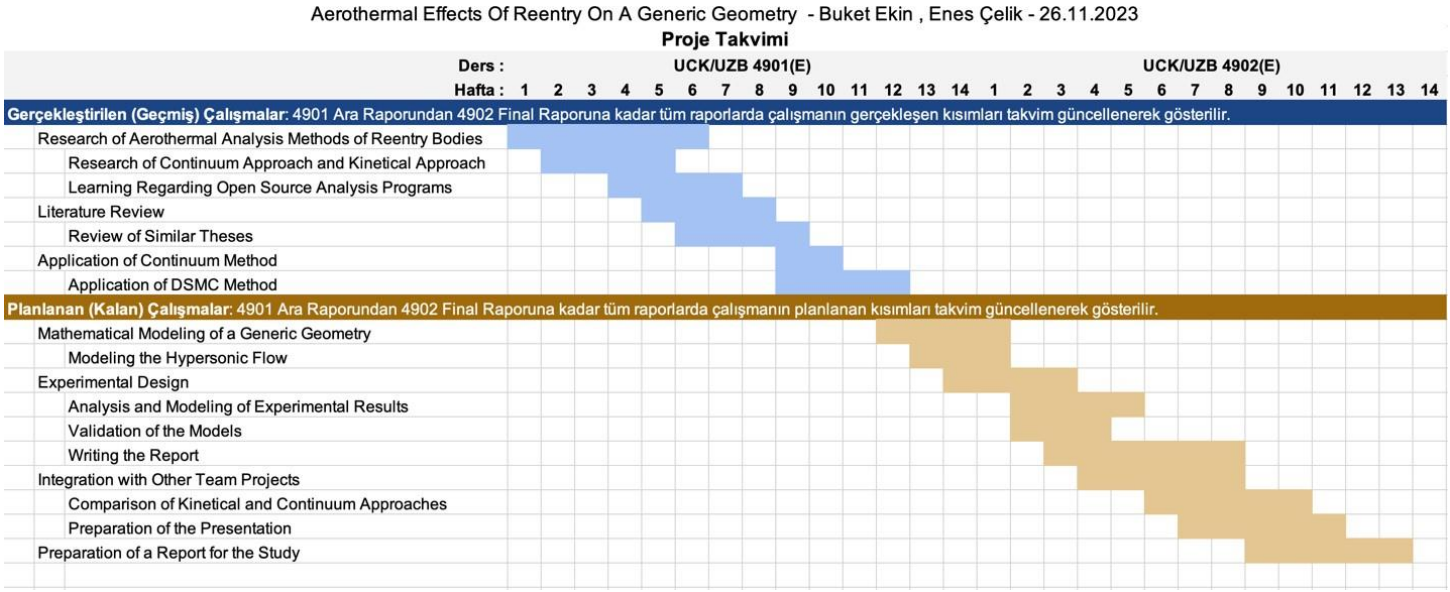

B. Team Form

UCK/UZB 4901(E)/4902(E) Bitirme ProjesiTakım Çalışması Formu Belge Tarihi: 23.01.2022, Sürümü: 0.2			
Öğrenci Adı Soyadı:	Enes Celik		
Öğrenci Numarası:	110180112		
Bitirme Projesi Başlığı:	Aerothermal Effects Of Reentry On A Generic Geometry – A Continuum Approach		
Bitirme Projesi Konusu:	Examination of aerodynamic heating at the entrance of the atmosphere with the Continuum Method		
Takım ÇalışmasınınBaşlığı, Konusu:	Aerothermal Effects Of Reentry On A Generic Geometry Examination and comparison of aerodynamic heating at atmospheric entry with continuous approach and kinetic-based approach		
Diğer TakımÜyelerinin Bilgileri:	**Diğer Takım Üyelerinin Bitirme ProjeBaşlıkları**	**İlgili Takım Üyesinin Bu ProjeninGerçekleşmesi için Sağlayacağı Çıktılar**	**Çıktıların Sağlanamaması Durumunda AlternatifÇözüm**
Buket Ekin	Aerothermal Effects Of Reentry On AGeneric Geometry – A Kinetic Approach	Will make a DSMC based approach using the Sparta Program	The results can be tried again with a higher capacity computer.
Danışman Onayı:			
Varsa Eş DanışmanOnayı:			

C.Statements of Ethic

-The student declares by signing the form that he/she has not committed any action that could be considered plagiarism.

-The scope of plagiarism evaluation includes scientific sources, technical documents, textbooks, patents, theses and especially previous graduation project reports.

-After delivery, some reports selected by random sampling may be checked for plagiarism (Turnitin, etc.). If an amount of unethical citation is detected above a threshold to be determined later, the student whose report is checked will fail the course. The results can be tried again with a high-capacity computer.

References

1. Maier, Walter T., et al. "SU2-NEMO: An Open-Source Framework for High-Mach Nonequilibrium Multi-Species Flows." Aerospace, vol. 8, no. 7, 2021, p. 193.
2. Cheatwood, F. M., and Peter A. Gnoffo. User's Manual for the Langley Aerothermodynamic Upwind Relaxation Algorithm (LAURA). NASA Technical Memorandum 4674, National Aeronautics and Space Administration, Langley Research Center, 1996.
3. Wright, Michael J., Graham V. Candler, and Deepak Bose. "Data-Parallel Line Relaxation Method for the Navier–Stokes Equations." AIAA Journal, vol. 36, no. 9, 1998, pp. 1603-1609.
4. Wright, Michael J., Todd White, and Nancy Mangini. Data Parallel Line Relaxation (DPLR) Code User Manual: Acadia - Version 4.01.1. NASA Technical Memorandum NASA/TM–2009-215388, Ames Research Center, 2009.
5. Candler, Graham V., et al. "Development of the US3D Code for Advanced Compressible and Reacting Flow Simulations." 53rd AIAA Aerospace Sciences Meeting, 5-9 January 2015, Kissimmee, Florida, AIAA 2015-1893, 2015.
6. Nompelis, I.; Drayna, T.; Candler, G. Development of a Hybrid Unstructured Implicit Solver for the Simulation of Reacting Flows Over Complex Geometries. In Proceedings of the 34th AIAA Fluid Dynamics Conference and Exhibit, Portland, OR, USA, 28 June–1 July 2004; p. 2227
7. Casseau, Vincent, Daniel E. R. Espinoza, Thomas J. Scanlon, and Richard E. Brown. "A Two-Temperature Open-Source CFD Model for Hypersonic Reacting Flows, Part Two: Multi-Dimensional Analysis." Aerospace, vol. 3, no. 4, 2016, p. 45.
8. Tay, Wee Beng, J.M. Li, C.J. Teo, B.C. Khoo, and X.Y. Zhang. "Validation of OpenFOAM and hy2Foam in Hypersonic Flow Simulations." Conference Paper, January 2019.
9. Lani, Andrea, et al. "The COOLFluiD Framework: Design Solutions for High-Performance Object-Oriented Scientific Computing Software." *Computational Science – ICCS 2005: 5th International Conference, Atlanta, GA, USA, May 22-25, 2005, Proceedings, Part I*, edited by Vaidy S. Sunderam, et al., Springer, 2005, pp. 279-287. Springer.
10. Economon, Thomas D., et al. "SU2: An Open-Source Suite for Multiphysics Simulation and Design." AIAA Journal, vol. 54, no. 3, 2016, pp. 828-846.
11. Maier, W., Needels, J. T., Alonso, J. J., Morgado, F., Garbacz, C., Fossati, M., Tumuklu, O., & Hanquist, K. M. (2023). Development of Physical and Numerical Nonequilibrium Modeling Capabilities within the SU2-NEMO Code. In AIAA Aviation *2023 Forum* Article 3488
12. Karl, Sebastian, Jan Martinez Schramm, and Klaus Hannemann. "High Enthalpy Cylinder Flow in HEG: A Basis for CFD Validation." 33rd AIAA Fluid Dynamics Conference and Exhibit, 23-26 June 2003, Orlando, Florida. AIAA 2003-4252. American Institute of Aeronautics and Astronautics, 2003.
13. Knight, Doyle, et al. "Assessment of CFD Capability for Prediction of Hypersonic Shock Interactions." *Progress in Aerospace Sciences*, vol. 48-49, 2012, pp. 8-26
14. Wang, Xiaoyong, Qizhen Hong, Yuan Hu, and Quanhua Sun. "On the Accuracy of Two-Temperature Models for Hypersonic Nonequilibrium Flow." *Acta Mechanica Sinica*, vol. 39, 2023, p. 122193. Springer
15. Park, C. Nonequilibrium Hypersonic Aerothermodynamics; Wiley: New York, NY, USA, 1990.